N-ethylmaleimide-sensitive factor siRNA inhibits the release of Weibel-Palade bodies in endothelial cells

YONG ZHOU[1], SHUI-XIANG YANG[2], YU-NAN YUE[2], XIAO-FEI WEI[2] and YAN LIU[3]

[1]Department of Cardiology; [2]Emergency Department, Beijing Shijitan Hospital, Capital Medical University, Beijing 100038; [3]Emergency Department, The 302 Hospital of People's Liberation Army, Beijing 100039, P.R. China

Received April 18, 2015; Accepted April 1, 2016

DOI: 10.3892/mmr.2016.5372

Abstract. The aim of the present study was to examine the effect of small interfering RNA (siRNA) methods on the expression of N-ethylmaleimide sensitive factor (NSF) and Weibel-Palade body (WPB) release in endothelial cells. A small hairpin RNA (shRNA), mediated with an adenovirus vector, was designed to target the N-terminal functional area of NSF. Subsequently, viruses were transfected into human aortic endothelial cells. The mRNA and protein expression levels of NSF were detected using reverse transcription-quantitative polymerase chain reaction and Western blot analyses, respectively, and the release of WPBs in the endothelial cells was examined using immunofluorescence. The mRNA expression of NSF in the endothelial cells, which were transfected with the adenoviruses carrying the NSF-shRNA was significantly decreased, compared with the negative control group (P=0.035) and blank control group (P=0.02). In addition, the mRNA expression of NSF was gradually decreased as duration increased; there were marked differences between the 24, 48 and 72 h groups (P<0.05). The protein expression of NSF was significantly decreased in the experimental group, compared with the negative control group (P=0.004) and blank control group (P=0.031), however, no difference was observed between the negative control and blank control groups (P=0.249). The immunofluorescence staining showed that the release of WPBs in the endothelial cells induced with thrombin was inhibited markedly following transfection with the virus carrying the NSF-shRNA. Therefore NSF-siRNA inhibited the mRNA and protein expression levels of NSF, and inhibited the release of WPBs in endothelial cells induced with thrombin. These results suggested that NSF-siRNA may be valuable for preventing and treating atherosclerosis and acute coronary syndrome.

Correspondence to: Dr Shui-Xiang Yang, Emergency Department, Beijing Shijitan Hospital, Capital Medical University, 10 Tieyi Road, Yangfangdian, Haidian, Beijing 100038, P.R. China
E-mail: yshuixiang_x@163.com

Key words: N-ethylmaleimide-sensitive factor, RNA interference, endothelial cell, Weibel Palade Body

Introduction

Due to their high rates of incidence and mortality, cardiovascular diseases have become a primary health concern worldwide, and increasing attention has focussed on the prevention and treatment of cardiovascular diseases.

The release of Weibel-Palade bodies (WPBs) in endothelial cells is associated with the occurrence and development of several types of heart disease, including atherosclerosis and acute coronary syndrome (1-3). N-ethylamaleimide-sensitive factor (NSF) is a key protein in the process of WPB membrane fusion with cell membranes, leading to the release of WPBs (4,5). Small interfering RNA (siRNA) can be used to repress the expression of specific target genes (6,7). Reports on the use of siRNA to inhibit the expression of NSF, to then downregulate WPB release, are limited. In the present study, small hairpin RNA (shRNA) was designed, which exhibited complimentary matching to the functional region of the NSF gene, to examine the mechanism of WPB release, based on previous investigations of NSF (8,9). The aim of the present study was to establish whether NSF-shRNA may offer a valuable method for the prevention and therapy of atherosclerosis and coronary heart disease, and for the results to provide a valuable reference in this.

Materials and methods

Design and synthesis of NSF-specific shRNA. RNA-Seq and Hierarchical Indexing for Spliced Alignment of Transcripts (HISAT) was used for analyzing the NSF sequence. The sequence of the human NSF gene was selected from the GeneBank database (http://www.insdc.org; gene accession no. NM_006178), and a 21 nt interference oligonucleotide sequence (5'-TAGGACTGGTTGTTGGAAACA-3'; https://rnaidesigner.thermofisher.com/rnaiexpress/) was used to target the N'-terminal region of the NSF gene using siRNA Target Designer-Version 1.51 software.

Two single strands encoding NSF-shRNA DNA were synthesized by GenePharma Co., Ltd. (Suzhou, China). followed by the termination sites of RNA polymerase III. The restriction enzyme sites, *Mlu*I and *Hind*III (Thermo Fisher Scientific, Inc., Waltham, MA, USA), were located at the ends of the strands.

NSF-shRNA adenovirus expression vector construction and identification. The pRNAT-H1.1/Adeno (SD1219; Thermo Fisher Scientific Inc.) adenovirus vector was digested using *Mlu*I and *Hind*III restriction enzymes. Following identification by agarose gel electrophoresis and purification, the vector was connected to the NSF-shRNA DNA template, which contained *Mlu*I and *Hind*III enzyme loci. 1% Agarose gel (Gene Company Ltd., Hong Kong, China) was prepared and used for electrophoresis for analysis of NSF-shRNA products. The results were recorded using a gel imaging system (Tanon 1600, Tanon Science & Technology Co., Ltd., Shanghai, China). The purification of NSF-shRNA was conducted using a DNA purification kit (Thermo Fisher Scientific Inc.), according to the manufacturer's instructions. Ligation of the products was performed by incubating 10 μl of reaction solution containing 50 ng of the annealed products, 1.5 μl of 10X T4 buffer (Thermo Fisher Scientific Inc.) and 0.5 μl T4 DNA ligase (Thermo Fisher Scientific Inc.) at 16˚C overnight. The recombinant vector was transformed into 50 μl DH5α-competent cells (American Type Culture Collection, Rockville, MD, USA). These cells (1x10^6 cells/ml) were inoculated into 400 μl lysogeny broth (Guangdong Huankai Microbial Sci & Tech., Co., Ltd. Guangzhou, China) supplemented with kanamycin in an incubator overnight (16-18 h) with agitation, at 37˚C. Following incubation, the DNA plasmids were extracted using a Plasmid DNA Mini-Preparation kit (Thermo Fisher Scientific Inc.), according to the manufacturer's protocol, and identified using 1% agarose gel electrophoresis. Following identification and sequencing, the plasmid was stored at -80˚C.

Viral packaging and preparation. Conventional resuscitation and subculture of HEK293 cells (American Type Culture Collection) were performed until 80% of the cells were fused. The cells were prepared by seeding 2x10^6-2x10^7 cells/ml into 24-well plates, with each well containing 0.5 ml cell suspension Dulbecco's modified Eagle's medium (DMEM, Gibco, Thermo Fisher Scientific Inc.) containing 10% fetal bovine serum (Gibco, Thermo Fisher Scientific Inc.). Transfection of the cells with the vector was performed using Lipofectamine 2000 (Thermo Fisher Scientific, Inc.) transfection reagent. Briefly, 80 μg DNA and 2 μl Lipofectamine 2000 were added to 50 μl serum-free DMEM. Following gentle mixing, the mixture was incubated at room temperature for 20 min., following which a further 1,000 μl DMEM was added to the DNA-Lipofectamine 2000 mixture. After 30 min, the mixture was used for transfection of the HEK293 cells. At 10 days post-transfection, the virus was released from the cells using a repeated freeze-thaw method, and stored at -80˚C.

Viral titer 50% tissue culture infective dose (TCID50) analysis. HEK293 cells (10 ml; 5x10^6) and 0.5 ml of the primitive viral presentation solution were added to a culture bottle at 37˚C in 5% CO_2 for 90 min, and 5% (9 ml) DMEM was added. After 72 h, the cells were collected and centrifuged at 600 x g for 5 min, and the supernatant was discarded. Subsequently, virus preservation solution (1 ml) was added and freeze-thawing was repeated three times at -20 and 37˚C. The supernatant was collected by centrifugation at 1,000 x g for 5 min. Using the TCID50 method for the measurement of viral interference, the pRNAT-H1.1 (SD1219) adenovirus vector carrying a cGFP gene was transduced into the HEK293 cells at concentrations of 1, 0.1, 0.01 and 0.001 μl respectively. Infected cells carrying the GFP tag, were green under the fluorescent microscope (XSP-63B, Shanghai Optical Instrument Factory, Co., Ltd., Shanghai, China). The number of green cells was calculated according to Reed-Muench or Karber methods. After 48 h, the effects were observed using a fluorescent microscope. In addition, QBC939 cells (1x10^6 cells/ml; American Type Culture Collection) were transduced with the recombinant adenovirus at 37˚C and 5% CO_2. Fluorescence polymerase chain reaction (PCR) analysis was used to detect the viral interference efficiency, and cells were frozen at -80˚C following assessment.

Transduction of human aortic endothelial cells (HAECs). HAECs (1x10^6 cells/ml; American Type Culture Collection) were transduced using Lipofectamine 2000 at 37˚C and 5% CO_2. The HAECs were plated in 6-well plates and allowed to grow to 70% confluence. Subsequently, 60 μl viral preservation solution was added to each well, periodically, at 0, 24, 48 and 72 h following administration of each sample. The NSF-shRNA adenovirus-transduced group was considered the experimental group, whereas the negative control group was transduced with the SD1219 adenovirus vector, and the blank control group was without interference.

Detection of target gene expression by reverse transcription-quantitative PCR (RT-qPCR) analysis.

Extraction of total RNA. Total RNA was isolated using TRIzol reagent (Sigma-Aldrich, St. Louis, MO, USA). Each group of cells were mixed with 200 μl reagent at 4˚C, and centrifuged at 8,000 x g for 5 min. The supernatant was discarded, and 50 μl H_2O-dissolved RNA was added at 55-60˚C for 5-10 min. The RNA concentration was quantified by measuring the absorbance, and total RNA was detected using electrophoresis.

Designation and synthesis of primers. According to the NSF mRNA sequence, the PCR primers were as follows: Upstream, TGGGCTGGGCTTTCTATTG; downstream, TGCCATCTT GTCGGTGTCA; with a PCR amplification fragment length of 150 bp. β-actin was used as a reference and had the following sequences: Upstream primer, TGACGTGGACATCCGCAA AG; downstream primer, CTGGAAGGTGGACAGCGAGG; with a PCR amplification fragment length of 205 bp. The primers were synthesized by Shanghai Shinegene Molecular Biotech, Inc. (Shanghai, China).

Quantification of mRNA levels of NSF. The entire process of RT-qPCR was monitored through real time fluorescent signal accumulation. All reactions were completed using the PCR System (StepOnePlusTM, Applied Biosystems, Thermo Fisher Scientific, Inc.). The 50 μl reaction mixture contained the following: 4 μl cDNA was, 1 μl primers, 4 μl dNTPs, 0.5 μl PCR enzyme, and 5 μl PCR buffer (Thermo Fisher Scientific Inc.). The reverse transcription step was conducted under the following conditions: 25˚C for 10 min, 42˚C for 60 min and 85˚C for 5 min, followed by cooling at 4˚C. By detecting the signals of the experimental group, negative control group and blank control group at 0, 24, 48 and 72 h, the relative gene expression levels were calculated, using the following method: ΔCq (relative expression) = Cq (gene)-Cq (internal reference) (10). The procedures were performed in accordance with the kit protocol.

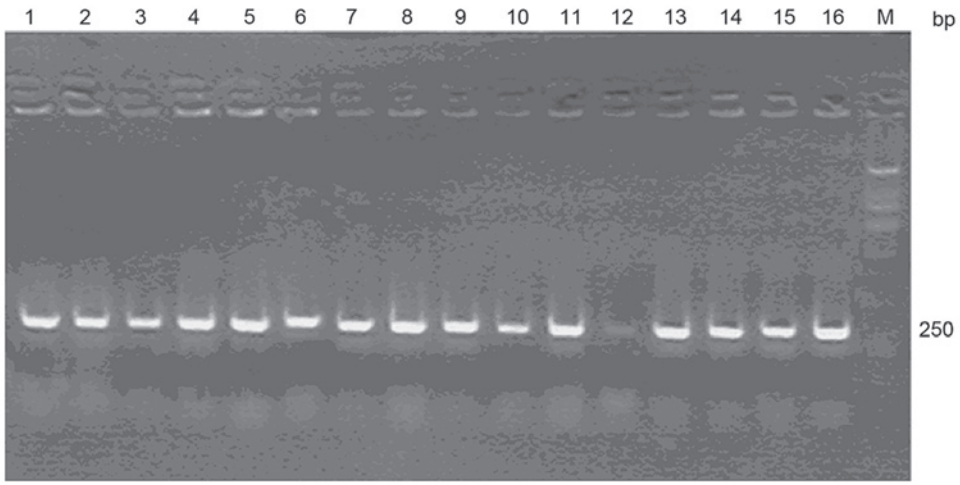

Figure 1. Polymerase chain reaction products of the recombinant adenovirus vector. Lanes 1-11 and 13-16 are positive clones. The size of the amplification bands is ~250 bp. Lane 12 is a negative clone, for which no amplification bands emerged.

The reaction conditions were as follows: 25˚C for 10 min, 42˚C for 60 min, 85˚C for 5 min and 4˚C cooling. The fluorescence qPCR amplification conditions were as follows: 35 cycles of 94˚C for 4 min, 60˚C for 30 sec and 72˚C for 30 sec, with β-actin as an internal reference, this was repeated three times and the average of the recorded Cq1, Cq2, Cq3 values was calculated .

Western blot analysis. The cells were digested and the proteins were extracted with radioimmunoprecipitation assay buffer (Beijing Solarbio Science and Technology Co., Ltd., Beijing, China). The quantity of the protein was confirmed by a bicinchoninic acid protein assay kit (Beyotime Institute of Biotechnology, Shanghai, China). The cells were washed in PBS (3 ml; 4˚C; 0.01 mol/l; pH 7.2-7.3) and homogenized in Triton-based lysis buffer (Wuhan Boster Biological Technology, Ltd., Wuhan, China). Equal quantities of protein (10 μl) were separated by sodium dodecyl sulfate polyacrylamide gel electrophoresis and transferred onto a nylon membrane (Merck KGaA, Darmstadt, Germany). Following blocking with 5% bovine serum albumin (GenView Scientific, Inc., Jacksonville, FL, USA), the membranes were incubated with rabbit polyclonal anti-NSF antibody (1:5,000, cat. no. 87155; Abcam, Cambridge, MA, USA) and rabbit anti-glyceraldehyde 3-phosphate dehydrogenase (GAPDH; 1:10,000, cat. no. 10494-1-AP, Proteintech Group Inc., Wuhan, China) primary antibodies overnight at 4˚C. Membranes were then incubated with goat anti-rabbit secondary antibody (1:3,000, cat. no. 111-035-003, Jackson ImmunoResearch Laboratories, Inc., West Grove, PA, USA) was used as secondary antibody. The membrane-bound antibodies were visualized by incubation with horseradish peroxidase-conjugated secondary antibodies (1:1,000 dilution) at 25˚C for 1 h. The membrane was visualized using an enhanced chemiluminescence system (Merck KGaA) and X-ray film (FUJIFILM (China) Investment Co., Ltd., Shanghai, China). The expression levels were quantified by densitometry.

Immunofluorescence staining. Immunofluorescence analysis of the transfected cells was performed 72 h following transfection. The cells were washed with PBS and cultivated with 4 U/l thrombin (Beijing Solarbio Science and Technology Co., Ltd.) for 1 h. The permeabilized cells were then incubated (at 25˚C) with a mouse anti-VWF antibody (1:1,000) in PBS for 1 h at room temperature. Following washing with PBS, the cells were incubated with a fluorescein isothiocyanate-conjugated anti-mouse IgG antibody for 1 h at room temperature. The cells were then observed using a Leica AF7000 fluorescence microscope (Leica Microsystems GmbH, Wetzlar, Germany) following washing with PBS, with data expressed as the mean ± standard deviation of three independent experiments.

Statistical analysis. Data are presented as the mean ± standard deviation. A homogeneity test of variance was performed using SPSS 16.0 statistical software (SPSS, Inc., Chicago, IL, USA). If variances were uneven, variable conversion was performed to reach homogeneity. Student's t-test was used for inter-group comparisons. $P<0.05$ was considered to indicate a statistically significant difference.

Results

Identification of NSF-shRNA sequences. The interfering oligonucleotide sequence targeting the N-terminal region of the NSF gene was designed as 5'-TAGGACTGGTCG TTGGAAACA-3' (21 nt). Following database analysis, no homologous sequences with other molecules were identified. The content of guanylate and cytosine was close to 50%. The positive and antisense strands were connected with a looped oligonucleotide (10 nt) to constitute shRNA. The sequences of NSF-shRNA had *Mlu*I and *Hind*III enzyme loci at the 5' and 3' terminals.

Sequencing results of the NSF-shRNA recombinant adenovirus vector. The products of the NSF-shRNA sequences were connected to the adenovirus vector, pRNAT-H1.1/Adeno (SD1219), and eukaryotic plasmid positive clones were established. Sequencing data were confirmed by sequence alignment results. Electrophoresis was used for identification of the PCR

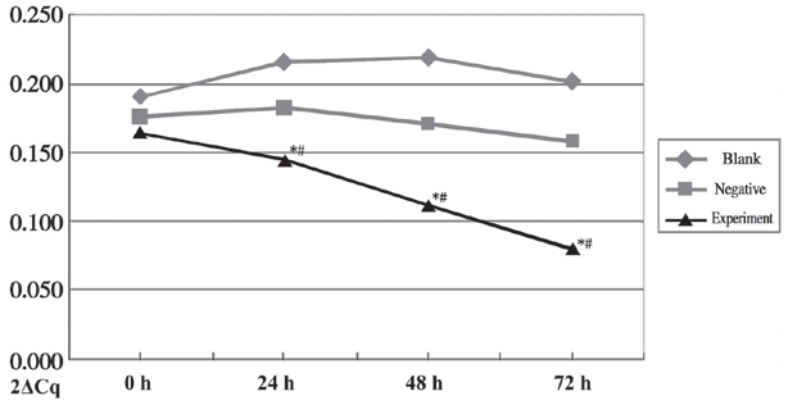

Figure 2. Changes in mRNA expression levels of NSF over time. NSF, N-ethylmaleimide sensitive factor. *P<0.05, compared with the negative control at the corresponding time point; #P<0.05, compared with the blank control at the corresponding time point.

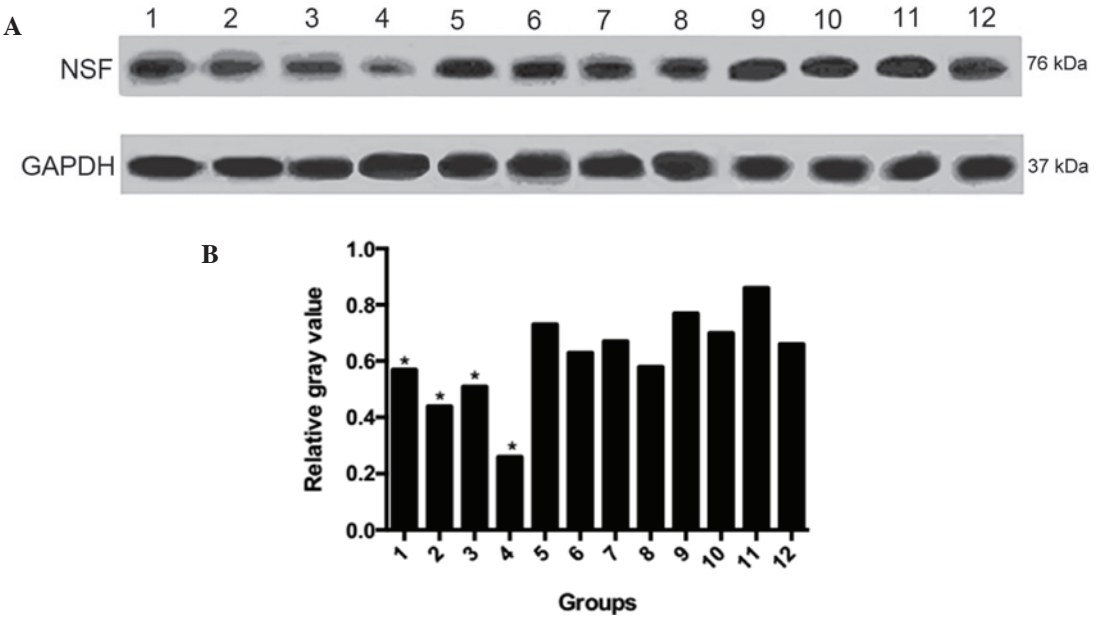

Figure 3. Protein expression levels of NSF. (A) Western blot analysis of NSF protein. (B) Relative gray values. Lane 1, experimental group 0 h; 2, experimental group 24 h; 3, experimental group 48 h; 4, experimental group 72 h; 5, negative control 0 h; 6, negative control 24 h; 7, negative control 48 h; 8, negative control 72 h; 9, blank control 0 h; 10, blank control 24 h; 11, blank control 48 h; 12, blank control 72 h. GAPDH served as the internal control. NSF, N-ethylmaleimide sensitive factor; GAPDH, glyceraldehyde 3-phosphate dehydrogenase. *P<0.05 compared with the negative control.

products, which showed that the sizes of the positive clones in the 1-11 and 13-16 lanes were ~250 bp. No specific amplification bands of the negative clone were identified (Fig. 1). The specific primers were as follows: Sense 5'-TAATACGAC TCACTATAGGG-3' and antisense 5'-CAAAACTACATA AGACCCCCAC-3'.

Identification of the recombinant adenovirus. The numbers of fluorescent cells were counted under an inverted microscope. The TCID50 value was determined using a classical method and the viral titer of recombinant adenovirus was determined to be $2x10^9$ TU/ml.

Detection of NSF mRNA. The total RNA in the purified samples were detected using an ultraviolet spectrophotometer, the optical density (OD)260/OD280 value was ~1.8-2.0. The bands of 18S/28S were bright and clear.

mRNA expression levels of NSF. The mRNA expression of NSF in the experimental group was markedly reduced and showed statistical difference, compared with the negative control group (P=0.035) and blank control group (P=0.02). The mRNA levels of NSF did not differ significantly in the negative or blank groups between the time points. In the experimental group, the mRNA level of NSF decreased in a time-dependent manner, with differences between the 24, 48 and 72 h groups (P<0.05; Fig. 2).

Protein expression of NSF. The protein expression of NSF was significantly decreased in the experimental group, compared with the negative control group (P=0.004) and blank control group (P=0.031), and the decreased protein expression level of NSF in the experimental group occurred in a time-dependent manner. No changes were observed in the protein levels of NSF and GAPDH in the blank and

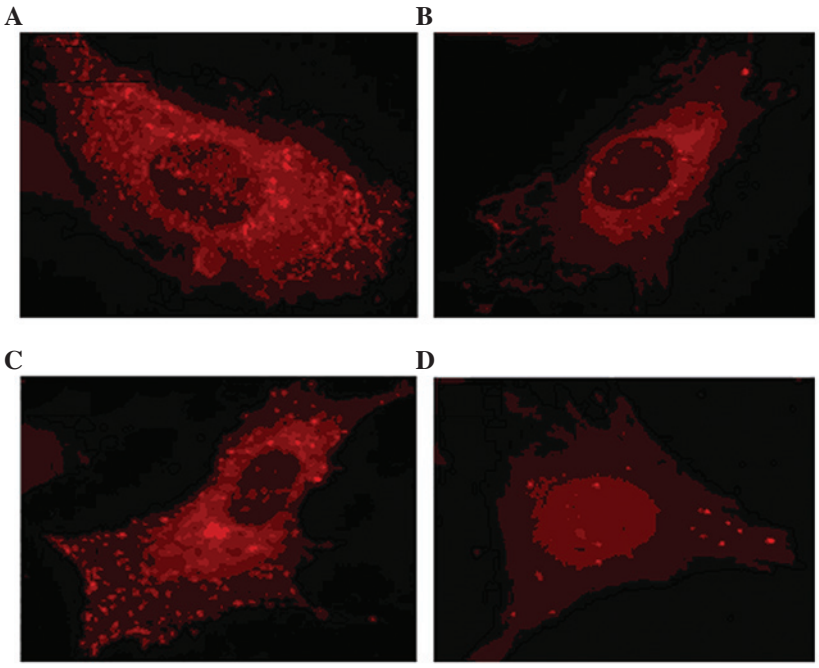

Figure 4. shRNA represses the release of WPB in human aortic endothelial cells. (A) Control group; (B) thrombin-induced WPB release; (C) shRNA+thrombin. shRNA repressed thrombin-induced WPB release; (D) dsDNA+thrombin, dsDNA did not repress thrombin-induced WPB release. Magnification, x60. WPB, Weibel-Palade body; shRNA, short hairpin RNA; ds, double stranded RNA.

negative control groups, and no statistical differences were observed between the blank and negative control groups (P=0.249; Fig. 3).

Fluorescence observation of WPB release following infection with shRNA. The immunofluorescence staining showed that the release of WPBs in the thrombin-induced endothelial cells was markedly inhibited following transduction with the virus carrying NSF-shRNA, but was not affected in the negative or blank control groups (Fig. 4).

Discussion

Using siRNA for the interference and silencing of genes has become an area of investigations in clinical treatment (11,12). In the present study, following the introduction of a recombinant adenovirus vector, the expression of NSF was downregulated in HAECs, indicating that NSF-shRNA inhibited WPB release.

Palade and de Duve first observed the release of WPB particles from human endothelial cells using immunoelectron microscopy. There are several bioactive substances present in WPBs, including P-selectin, endothelin-1 (ET-1) and interleukin-8 (IL-8). The elevation of P-selectin reflects endogenous platelet activation (13). ET-1 is a vasoconstrictor peptide, which can cause coronary vasospasm and may lead to myocardial ischemia (14). IL-8, as one of the leukocyte chemoattractants, stimulates the activation of leukocyte integrins (15). Therefore, the release of WPBs leads to platelet aggregation, which may cause the adhesion of neutrophils to the vascular endothelium and result in vasospasm. A series of inflammatory reactions occur at the blood vessel wall, and this pathophysiological process is closely associated with atherosclerosis and acute coronary syndrome (16).

NSF was first identified as a cytosolic protein, which is necessary for the *in vitro* reconstitution of Golgi transportation, and has been subsequently shown to regulate intracellular transport in several species (17-19). Soluble NSF receptor (SNARE) proteins, which are localized to vesicle and target membranes, assemble into stable ternary complexes. NSF and the family of soluble NSF attachment proteins (SNAPs), are critical in regulating vesicle trafficking by hydrolyzing ATP and disassembling SNARE. NSF comprises three domains: An N-terminal domain and two homologous ATP binding domains. The N-terminal domain (residues 1-205) interacts with members of the SNAP family, which in turn interact with SNARE molecules (20).

As WPBs are critical in the regulation of cardiovascular diseases, the present study aimed to identify methods to inhibit NSF in order to regulate the release of WPBs. A report by Lowenstein *et al* suggested that thioredoxin increases exocytosis by denitrosylating NSF (5). Nitric oxid inhibits the platelet secretion of granules by targeting NSF, leading to diverse effects in inhibiting thrombosis and limiting vascular inflammation (8). Three specific SNAREs molecules, vesicle-associated membrane protein (VAMP)-1, VAMP-2 and syntaxin-4, regulate cardiac myocyte exocytosis of atrial natriuretic peptide, which may affect natriuresis and blood pressure (21,22). Circulating levels of ET-1 are increased by NSF in aged arteries (23). In our previous study, it was confirmed that in addition to the increase in WPBs mediated by thrombin, the binding activity of Rac-GTP and reactive oxygen species (ROS) were upregulated. The expression mechanism of WPBs was regarded as an Rac1-dependent ROS regulatory process (9). Therefore, the present study examined how NSF siRNA inhibits the release of WPBs.

An important finding of the present study was that the transcription of NSF mRNA in the experimental group

decreased significantly, compared with the blank and negative control groups, with similar results for NSF protein. This result demonstrates that RNA interference (RNAi) induced by NSF-shRNA repressed target gene expression.

Following the transduction of HASCs with a recombinant adenovirus, shRNAs are amplified under the control of a recombinant adenovirus H1 promoter. shRNA is cleaved to yield siRNA, which targets NSF. The NSF-siRNA duplex is unwound to form the RNA-induced silencing complex, which recognizes target mRNA. Target recognition is dependent on complementarity to the target region. Finally, translational inhibition or, in certain cases, mRNA degradation, contributes to downregulation in the mRNA level of NSF. At the same time, the gene encoding the N-terminal functional region of NSF is inactivated, SNARE compounds cannot depolymerize, and WPB release is inhibited.

Previous investigations have demonstrated that vector-based RNAi has time- and dose-dependent effects in mammalian cells, and observed that decreases in mRNA or protein levels were not marked at 12 h, but gradually became more evident between 24 and 48 h. The decrease reached a maximal degree between 48 and 60 h, and then became less marked prior to being restored (24). The reason for this may be due to viral replication interference by cell division. The efficiency of RNAi had a similar time-dependent effect in the present study. In the experimental group, the mRNA and protein levels of NSF declined gradually as the duration of co-culture increased, and the maximum inhibition was observed 72 h following transfection. This may be affected by several factors, including transfection efficiency, co-culture duration, cell type and quantity of vector.

In conclusion, the present study demonstrated the inhibition of WPB release in endothelial cells with siRNA, mediated by a recombinant adenovirus. The biology of RNAi represents a relatively novel area of research. However, further investigations are required prior to the use of RNAi-based therapeutic strategies in humans (25). The recombinant adenovirus components may induce immunoreactions in the host. The selection of an appropriate vector, helper virus or plasmid, and the viral purification and biosecurity are major challenges, although RNAi may offer an effective strategy in the treatment of cardiovascular diseases.

Acknowledgements

The current study was supported by the Beijing Natural Science Foundation (grant no. 7083108).

References

1. Valentijn KM, van Driel LF, Mourik MJ, Hendriks GJ, Arends TJ, Koster AJ and Valentijn JA: Multigranular exocytosis of Weibel-Palade bodies in vascular endothelial cells. Blood 116: 1807-1816, 2010.
2. Kiskin NI, Hellen N, Babich V, Hewlett L, Knipe L, Hannah MJ and Carter T: Protein mobilities and P-selectin storage in Weibel-Palade bodies. J Cell Sci 123: 2964-2975, 2010.
3. Berriman JA1, Li S, Hewlett LJ, Wasilewski S, Kiskin FN, Carter T, Hannah MJ and Rosenthal PB: Structural organization of Weibel-Palade bodies revealed by cryo-EM of vitrified endothelial cells. Proc Natl Acad Sci USA 106: 17407-17412, 2009.
4. Lowenstein CJ and Tsuda H: N-ethylmaleimide-sensitive factor: A redox sensor in exocytosis. Biol Chem 387: 1377-1383, 2006.
5. Lowenstein CJ, Morrell CN and Yamakuchi M: Regulation of Weibel-Palade body exocytosis. Trends in Cardiovasc Med 15: 302-308, 2005.
6. Sioud M: Promises and challenges in developing RNAi as a research tool and therapy. Methods in Mol Biol 703: 173-187, 2011.
7. Shimizu H and Fujita T: New short interfering RNA-based therapies for glomerulonephritis. Nat Rev Nephrol 7: 407-415, 2011.
8. Qian Z, Gelzer-Bell R, Yang Sx SX, Cao W, Ohnishi T, Wasowska BA, Hruban RH, Rodriguez ER, Baldwin WM III and Lowenstein CJ: Inducible nitric oxide synthase inhibition of weibel-palade body release in cardiac transplant rejection. Circulation 104: 2369-2375, 2001.
9. Yang SX, Yan J, Deshpande SS, Irani K and Lowenstein CJ: Rac1 regulates the release of Weibel-Palade bodies in human aortic endothelial cells. Chin Med J (Engl) 117: 1143-1150, 2004.
10. Livak KJ and Schmittgen TD: Analysis of relative gene expression data using real-timequantitative PCR and the 2(-Delta Delta C(T)) Method. Methods 25: 402-408, 2001.
11. Ming X: Cellular delivery of siRNA and antisense oligonucleotides via receptor-mediated endocytosis. Expert Opin Drug Deliv 8: 435-449, 2011.
12. Samuel-Abraham S and Leonard JN: Staying on message: Design principles for controlling nonspecific responses to siRNA. FEBS J 277: 4828-4836, 2010.
13. Amin HM, Ahmad S, Walenga JM, Hoppensteadt DA, Leitz H and Fareed J: Soluble P-selectin in human plasma: Effect of anticoagulant matrix and its levels in patients with cardiovascular disorders. Clin Appl Thromb Hemost 6: 71-76, 2000.
14. Russell FD, Skepper JN and Davenport AP: Evidence using immunoelectron microscopy for regulated and constitutive pathways in the transport and release of endothelin. J Cardiovasc Pharmacol 31: 424-430, 1998.
15. Wolff B, Burns AR, Middleton J and Rot A: Endothelial cell 'memory' of inflammatory stimulation: Human venular endothelial cells store interleukin 8 in Weibel-Palade bodies. J Exp Med 188: 1757-1762, 1998.
16. Alberto P1, Francesca I, Chiara S and Ranuccio N: Acute coronary syndromes: from the laboratory markers to the coronary vessels. Biomark Insights 1: 123-130, 2007.
17. Ito T, Yamakuchi M and Lowenstein CJ: Thioredoxin increases exocytosis by denitrosylating N-ethylmaleimide-sensitive factor. J Biol Chem 1: 11179-11184, 2011.
18. Lowenstein CJ: Nitric oxide regulation of protein trafficking in the cardiovascular system. Cardiovasc Res 75: 240-246, 2007.
19. Ferlito M, Fulton WB, Zauher MA, Marbán E, Steenbergen C and Lowenstein CJ: VAMP-1, VAMP-2 and syntaxin-4 regulate ANP release from cardiac myocytes. J Mol Cell Cardiol 49: 791-800, 2010.
20. Matsushita K, Morrell CN, Cambien B, Yang SX, Yamakuchi M, Bao C, Hara MR, Quick RA, Cao W, O'Rourke B, *et al*: Nitric oxide regulates exocytosis by S-nitrosylation of N-ethylmaleimdide-sensitive factor. Cell 115: 139-150, 2003.
21. Yamakuchi M, Ferlito M, Morrell CN, Matsushita K, Fletcher CA, Cao W and Lowenstein CJ: Exocytosis of endothelial cells is regulated by N-ethylmaleimide-sensitive factor. Methods Mol Biol 440: 203-215, 2008.
22. Calvert JW, Gundewar S, Yamakuchi M, Park PC, Baldwin WM III, Lefer DJ and Lowenstein CJ: Inhibition of N-ethylmaleimide-sensitive factor protects against myocardial ischemia/reperfusion injury. Circ Res 101: 1247-1254, 2007.
23. Goel A, Su B, Flavahan S, Lowenstein CJ, Berkowitz DE and Flavahan NA: Increased endothelial exocytosis and generation of endothelin-1 contributes to constriction of aged arteries. Circ Res 107: 242-251, 2010.
24. Martinez J, Patkaniowska A, Urlaub H, Lührmann R and Tuschl T: Single-stranded antisense siRNAs guide target RNA cleavage in RNAi. Cell 110: 563-574, 2002.
25. Deng Y, Wang CC, Choy KW, Du Q, Chen J, Wang Q, Li L, Chung TK and Tang T: Therapeutic potentials of gene silencing by RNA interference: Principles, challenges and new strategies. Gene 538: 217-227, 2014.